Multi-stage Attention ResU-Net for Semantic Segmentation of Fine-Resolution Remote Sensing Images

Rui Li, Shunyi Zheng, Chenxi Duan, Jianlin Su, and Ce Zhang

***Abstract*—The attention mechanism can refine the extracted feature maps and boost the classification performance of the deep network, which has become an essential technique in computer vision and natural language processing. However, the memory and computational costs of the dot-product attention mechanism increase quadratically with the spatio-temporal size of the input. Such growth hinders the usage of attention mechanisms considerably in application scenarios with large-scale inputs. In this Letter, we propose a Linear Attention Mechanism (LAM) to address this issue, which is approximately equivalent to dot-product attention with computational efficiency. Such a design makes the incorporation between attention mechanisms and deep networks much more flexible and versatile. Based on the proposed LAM, we re-factor the skip connections in the raw U-Net and design a Multi-stage Attention ResU-Net (MAResU-Net) for semantic segmentation from fine-resolution remote sensing images. Experiments conducted on the Vaihingen dataset demonstrated the effectiveness and efficiency of our MAResU-Net. Open-source code is available at https://github.com/lironui/MAResU-Net.**

***Index Terms*—semantic segmentation, fine-resolution remote sensing images, linear attention mechanism**

I. Introduction

Attention mechanisms, benefiting from their powerful ability to exploit long-range dependencies of the feature maps and facilitate neural networks to explore global contextual information, are at the research forefront of computer vision (CV) and natural language processing (NLP). Dot-product attention mechanisms, generating response at each pixel by weighting features in the previous layer, expand the receptive field to the entire input feature maps in one pass. With a strong ability to capture long-range dependencies, dot-product attention mechanisms have been widely used in vision and language processing tasks. For example, dot-product-attention-based Transformer [4] has demonstrated state-of-the-art performance in nearly all tasks in NLP. The non-local module [6], dot-product-based attention for CV, has demonstrated its superiority on a wide range of vision tasks [5, 7].

However, as the memory and computational overhead of the dot-product attention mechanism increases quadratically, along with the spatio-temporal size of the input, it is difficult to model the global dependency on massive inputs, such as large-scale videos, long sequences, or fine-resolution images, thereby remaining an intractable problem [8]. To alleviate the huge computational costs, Child et al. [10] designed sparse factorizations of the attention matrix and reduce the complexity from $O(N^2)$ to $O(N\sqrt{N})$. Using locality sensitive hashing, Kitaev et al. [12] decreased the complexity to $O(N \log N)$. Furthermore, Katharopoulos et al. [13] and Li et al. [14] took self-attention as a linear dot-product of kernel feature maps, and Shen et al. [15] modified the position of softmax functions, resulting in the complexity reduction at $O(N)$.

In this Letter, we not only reduce the complexity of the dot-product attention mechanism to $O(N)$ from a novel facet, but also increase the classification performance of the U-Net by incorporating the proposed attention and ResNet-based backbones. Specifically, we take the ResNet-34 as the encoder and substitute the plain skip connections within the raw U-Net into our attention blocks at multiple stages, which refine the multi-scale feature maps captured by the network.

As an elaborate encoder-decoder architecture, U-Net [1] has demonstrated its great potential in various areas [16]. Generally, the encoder-decoder-based network includes a contracting part, i.e., encoder, that captures traits of the input and generates corresponding feature maps, and an expanding part, i.e., decoder, in which the mask for pixel-wise segmentation is reconstructed. Specifically, feature maps generated by the encoder are comprised of low-level and fine-grained detailed information, while those of the decoder contain high-level and coarse-grained semantic information [17]. The skip connections, which concatenate the low-level and high-level feature maps, have shown to be effective in enhancing the feature extraction capability of encoder-decoder frameworks. Nevertheless, the plain skip connections in the raw U-Net only connect the features without any further process, leading to insufficient utilization of the abundant information. Here, we design a multi-stage attention ResU-Net (MAResU-Net) to remedy this

This work was supported in part by the National Natural Science Foundations of China (No. 41671452). *(Corresponding author: Rui Li.)*

R. Li and S. Zheng are with School of Remote Sensing and Information Engineering, Wuhan University, Wuhan 430079, China (e-mail: lironui@whu.edu.cn; syzheng@whu.edu.cn).

Jianlin Su is with the Shenzhen Zhuiyi Technology Co., Ltd. (e-mail: bojonesu@wezhuiyi.com)

C. Duan is with the State Key Laboratory of Information Engineering in Surveying, Mapping, and Remote Sensing, Wuhan University, Wuhan 430079, China; chenxiduan@whu.edu.cn (e-mail: chenxiduan@whu.edu.cn).

C. Zhang is with Lancaster Environment Centre, Lancaster University, Lancaster LA1 4YQ, United Kingdom; UK Centre for Ecology & Hydrology, Library Avenue, Lancaster, LA1 4AP, United Kingdom (e-mail: c.zhang9@lancaster.ac.uk).

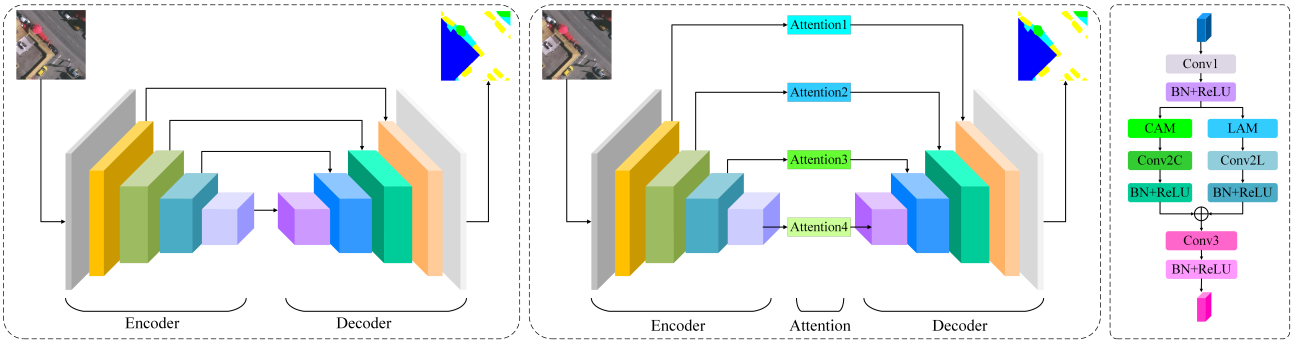

(a) The Structure of the Raw U-Net (b) The Structure of the Proposed MAResU-Net (c) The Attention Block

Fig. 1. The structure of (a) the raw U-Net, (b) the proposed MAResU-Net, and (c) the attention block.

limitation based on the proposed memory-saving and computation-effective linear attention mechanism (LAM). Experiments on Vaihingen semantic segmentation dataset manifest the effectiveness of the proposed network.

II. Related Works

A. Dot-Product Attention

To enhance word alignment in machine translation, Bahdanau et al. [18] proposed the initial formulation of the dot-product attention mechanism. Subsequently, recurrences are completely replaced by attention in Transformer [4]. The state-of-the-art records in almost all tasks in NLP demonstrate the superiority of the attention mechanism. Wang et al. [6] modified the dot-product attention for CV and proposed the non-local module. Other related work conducted on different tasks of CV further showed the effectiveness and general utility of the attention mechanism.

B. Semantic Segmentation

Fully Convolutional Network (FCN) based methods have witnessed enormous progress in semantic segmentation. DilatedFCN and EncoderDecoder are two prominent directions in FCN.

DilatedFCN The dilated or atrous convolution [19, 20] has shown its strong capability to retain the receptive field-of-view and enhance the performance of the backbone. Subsequent research concentrates on capture substantial contextual information, such as PSPNet [3] and DANet [5].

EncoderDecoder The EncoderDecoders utilize an encoder to capture multi-level feature maps, which are then incorporated into the final prediction by a decoder [1]. The refinement of the connection manners between the encoder and decoder [17] and the structure optimization based on residual connections are two significant directions [2].

C. Dot-Product Attention for Semantic Segmentation

Based on dot-product attention and its variants, substantial number of attention-based networks have been proposed to address the semantic segmentation problem. Inspired by the non-local module [6], Dual Attention Network (DANet) [5], Point-wise Spatial Attention Network (PSANet) [21], Object Context Network (OCNet) [22], and Co-occurrent Feature Network (CFNet) [23] have been proposed for scene segmentation by exploring the long-range dependency.

III. Methodology

A. Definition of Dot-Product Attention

Providing N and C as the length of input sequences and the number of input channels, where $N = H \times W$, and H and W denote the height and width of the input, with the input feature $\boldsymbol{X} = [\boldsymbol{x}_1, \cdots, \boldsymbol{x}_N] \in \mathbb{R}^{N \times C}$, dot-product attention utilize three projected matrices $\boldsymbol{W}_q \in \mathbb{R}^{D_x \times D_k}$, $\boldsymbol{W}_k \in \mathbb{R}^{D_x \times D_k}$, and $\boldsymbol{W}_v \in \mathbb{R}^{D_x \times D_v}$ to generate corresponding query matrix $\boldsymbol{Q}$, the key matrix $\boldsymbol{K}$, and the value matrix $\boldsymbol{V}$:

$$\begin{aligned} \boldsymbol{Q} &= \boldsymbol{X}\boldsymbol{W}_q \in \mathbb{R}^{N \times D_k}, \\ \boldsymbol{K} &= \boldsymbol{X}\boldsymbol{W}_k \in \mathbb{R}^{N \times D_k}, \\ \boldsymbol{V} &= \boldsymbol{X}\boldsymbol{W}_v \in \mathbb{R}^{N \times D_v}. \end{aligned} \tag{1}$$

Note the dimensions of the query matrix and key matrix have to be identical and all the vectors in this Letter are column vectors by default. A normalization function ρ evaluates the similarity between the i-th query feature $\boldsymbol{q}_i^T \in \mathbb{R}^{D_k}$ and the j-th key feature $\boldsymbol{k}_j \in \mathbb{R}^{D_k}$ by $\rho(\boldsymbol{q}_i^T \boldsymbol{k}_j) \in \mathbb{R}^1$. Generally, as the query feature and key feature are generated by diverse layers, the similarities between $\rho(\boldsymbol{q}_i^T \boldsymbol{k}_j)$ and $\rho(\boldsymbol{q}_j^T \boldsymbol{k}_i)$ are not symmetric. By calculating the similarities between all pairs of positions and taking the similarities as weights, the dot-product attention module computes the value at position i by aggregating the value features from all positions based on weighted summation:

$$D(\boldsymbol{Q}, \boldsymbol{K}, \boldsymbol{V}) = \rho(\boldsymbol{Q}\boldsymbol{K}^T)\boldsymbol{V}. \tag{2}$$

The softmax is taken as the common normalization function:

$$\rho(\boldsymbol{Q}\boldsymbol{K}^T) = softmax_{row}(\boldsymbol{Q}\boldsymbol{K}^T), \tag{3}$$

where $softmax_{row}$ indicates applying the softmax function along each row of matrix $\boldsymbol{Q}\boldsymbol{K}^T$.

The $\rho(\boldsymbol{Q}\boldsymbol{K}^T)$ models the similarities between each pair of pixels of the input, thoroughly extracting the global contextual information contained in the features. However, as $\boldsymbol{Q} \in \mathbb{R}^{N \times D_k}$ and $\boldsymbol{K}^T \in \mathbb{R}^{D_k \times N}$, the product between $\boldsymbol{Q}$ and $\boldsymbol{K}^T$ belongs to $\mathbb{R}^{N \times N}$, which leads to $O(N^2)$ memory and computational complexity. Therefore, the huge demand for resources in dot-product limits the application crucially on large inputs.

B. Generalization of Dot-Product Attention

Under the condition of softmax normalization function, the i-th row of result matrix generated by the dot-product attention module according to equation (2) can be written as:

$$D(\boldsymbol{Q},\boldsymbol{K},\boldsymbol{V})_i = \frac{\sum_{j=1}^{N} e^{\boldsymbol{q}_i{}^T \boldsymbol{k}_j}\boldsymbol{v}_j}{\sum_{j=1}^{N} e^{\boldsymbol{q}_i{}^T \boldsymbol{k}_j}}, \tag{4}$$

Equation (4) can then be generalized for any normalization function and rewritten as:

$$D(\boldsymbol{Q},\boldsymbol{K},\boldsymbol{V})_i = \frac{\sum_{j=1}^{N} \mathrm{sim}(\boldsymbol{q}_i,\boldsymbol{k}_j)\boldsymbol{v}_j}{\sum_{j=1}^{N} \mathrm{sim}(\boldsymbol{q}_i,\boldsymbol{k}_j)}, \quad \mathrm{sim}(\boldsymbol{q}_i,\boldsymbol{k}_j) \geq 0. \tag{5}$$

where $\mathrm{sim}(\boldsymbol{q}_i,\boldsymbol{k}_j)$ can be expanded as $\phi(\boldsymbol{q}_i)^T\varphi(\boldsymbol{k}_j)$ which measures the similarity between the $\boldsymbol{q}_i$ and $\boldsymbol{k}_j$. Specifically, if $\phi(\cdot) = \varphi(\cdot) = e^{(\cdot)}$, equation (5) is equivalent to equation (4). As a consequence, equation (4) can be rewritten as:

$$D(\boldsymbol{Q},\boldsymbol{K},\boldsymbol{V})_i = \frac{\sum_{j=1}^{N} \phi(\boldsymbol{q}_i)^T\varphi(\boldsymbol{k}_j)\boldsymbol{v}_j}{\sum_{j=1}^{N} \phi(\boldsymbol{q}_i)^T\varphi(\boldsymbol{k}_j)}, \tag{6}$$

and can be further simplified as:

$$D(\boldsymbol{Q},\boldsymbol{K},\boldsymbol{V})_i = \frac{\phi(\boldsymbol{q}_i)^T \sum_{j=1}^{N} \varphi(\boldsymbol{k}_j)\boldsymbol{v}_j{}^T}{\phi(\boldsymbol{q}_i)^T \sum_{j=1}^{N} \varphi(\boldsymbol{k}_j)}. \tag{7}$$

As $\boldsymbol{K} \in \mathbb{R}^{D_k \times N}$ and $\boldsymbol{V}^T \in \mathbb{R}^{N \times D_v}$, the product between $\boldsymbol{K}$ and $\boldsymbol{V}^T$ belongs to $\mathbb{R}^{D_k \times D_v}$, which reduces the complexity of the dot-product attention mechanism considerably.

C. Linear Attention Mechanism

Different from previous research, we conceive LAM based on the first-order approximation of Taylor expansion on equation (4):

$$e^{\boldsymbol{q}_i{}^T \boldsymbol{k}_j} \approx 1 + \boldsymbol{q}_i{}^T \boldsymbol{k}_j. \tag{8}$$

The above approximation, however, cannot guarantee the non-negativity. To ensure $\boldsymbol{q}_i{}^T \boldsymbol{k}_j \geq -1$, we can normalize $\boldsymbol{q}_i$ and $\boldsymbol{k}_j$ by l_2 norm:

$$sim(\boldsymbol{q}_i,\boldsymbol{k}_j) = 1 + \left(\frac{\boldsymbol{q}_i}{\|\boldsymbol{q}_i\|_2}\right)^T \left(\frac{\boldsymbol{k}_j}{\|\boldsymbol{k}_j\|_2}\right). \tag{9}$$

Then, equation (5) can be rewritten as:

$$D(\boldsymbol{Q},\boldsymbol{K},\boldsymbol{V})_i = \frac{\sum_{j=1}^{N} \left(1 + \left(\frac{\boldsymbol{q}_i}{\|\boldsymbol{q}_i\|_2}\right)^T \left(\frac{\boldsymbol{k}_j}{\|\boldsymbol{k}_j\|_2}\right)\right)\boldsymbol{v}_j}{\sum_{j=1}^{N} \left(1 + \left(\frac{\boldsymbol{q}_i}{\|\boldsymbol{q}_i\|_2}\right)^T \left(\frac{\boldsymbol{k}_j}{\|\boldsymbol{k}_j\|_2}\right)\right)}, \tag{10}$$

and can be simplified as:

$$D(\boldsymbol{Q},\boldsymbol{K},\boldsymbol{V})_i = \frac{\sum_{j=1}^{N} \boldsymbol{v}_j + \left(\frac{\boldsymbol{q}_i}{\|\boldsymbol{q}_i\|_2}\right)^T \sum_{j=1}^{N} \left(\frac{\boldsymbol{k}_j}{\|\boldsymbol{k}_j\|_2}\right)\boldsymbol{v}_j^T}{N + \left(\frac{\boldsymbol{q}_i}{\|\boldsymbol{q}_i\|_2}\right)^T \sum_{j=1}^{N} \left(\frac{\boldsymbol{k}_j}{\|\boldsymbol{k}_j\|_2}\right)}. \tag{11}$$

The above equation can be transformed into a vectorized form:

$$D(\boldsymbol{Q},\boldsymbol{K},\boldsymbol{V}) = \frac{\sum_j \boldsymbol{V}_{i,j} + \left(\frac{\boldsymbol{Q}}{\|\boldsymbol{Q}\|_2}\right)\left(\left(\frac{\boldsymbol{K}}{\|\boldsymbol{K}\|_2}\right)^T \boldsymbol{V}\right)}{N + \left(\frac{\boldsymbol{Q}}{\|\boldsymbol{Q}\|_2}\right)\sum_j \left(\frac{\boldsymbol{K}}{\|\boldsymbol{K}\|_2}\right)_{i,j}^T}. \tag{12}$$

As $\sum_{j=1}^{N} \left(\frac{\boldsymbol{k}_j}{\|\boldsymbol{k}_j\|_2}\right)\boldsymbol{v}_j^T$ and $\sum_{j=1}^{N} \left(\frac{\boldsymbol{k}_j}{\|\boldsymbol{k}_j\|_2}\right)$ can be calculated and reused for every query, time and memory complexity of the proposed LAM based on equation (12) is $O(N)$.

D. Multi-stage Attention ResU-Net

We design the attention block based on the proposed LAM to capture global contextual information, as shown in Fig 1(b). Considering the channels of the input C is normally far less than the number of pixels (i.e., $C \ll N$), the complexity of the softmax function for channels (i.e., $O(C^2)$), is not high based on equation (3). Thus, for the channel dimension, we directly harness dot-product-based attention.

As the complexity is dramatically decreased by the proposed LAM, the usage of the attention block for large feature maps is brought within the bounds of possibility. Thus, by taking the ResNet as the backbone, we design the MAResU-Net to combine the low-level and high-level feature maps through attention block in multiple stages, as shown in Fig 1(a). To design a concise but effective framework, we select the ResNet-18 and ResNet-34 as backbones rather than more complicated ResNets (e.g., ResNet-101).

IV. EXPERIMENTAL RESULTS

A. Dataset

The Vaihingen semantic labeling dataset [24] is composed of 33 tiles, with an average size of 2494 × 2064 pixels and a GSD of 5 cm. The near-infrared, red, and green channels together with DSM are provided in the dataset. There are 16 image tiles in the training set and 17 image tiles in the test set. Concretely, we exploit ID: 2, 4, 6, 8, 10, 12, 14, 16, 20, 22, 24, 27, 29, 31, 33, 35, 38 for testing, ID: 30 for validation, and the remaining 15 images for training. Please note that we do not use DSM in our experiments for simplicity.

B. Experimental Setting

All of the experiments are implemented with PyTorch on a single Tesla V100, and the optimizer is set as AdamW with a 0.0003 learning rate. The soft cross-entropy loss function is used as a quantitative evaluation, and a backpropagation index is adopted to measure the disparity between the obtained 2D segmentation maps and ground truth. For each method, the overall accuracy (OA), mean Intersection over Union (mIoU), and F1-score (F1) are chosen as evaluation indexes. OA is computed for all categories including the background.

C. Semantic Segmentation Results and Analysis

1) Performance Comparison: The experimental results of different methods on the Vaihingen dataset are demonstrated in Table I. The proposed MAResU-Net based on ResNet-34 achieves the highest mean F1-score of 90.277 %, OA of 90.860%, and mIoU of 83.301%, which is higher than recent contextual information aggregation methods designed initially for natural images, such as PSPNet and DANet, and also prevail over lastest multi-scale feature aggregation models proposed for remote sensing images, such as ResUNet-a and EaNet.

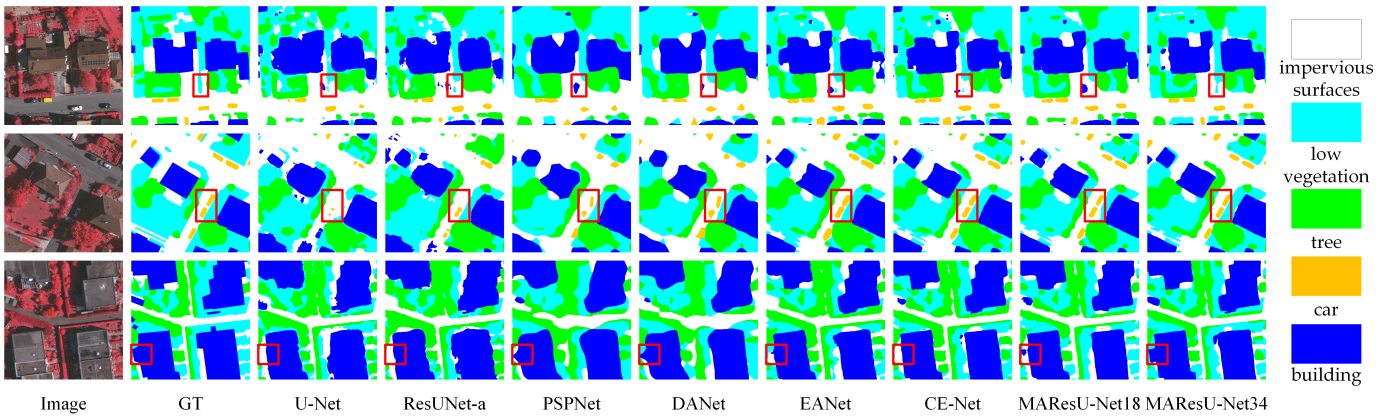

Fig. 2. Visualization of results on the Vaihingen.

TABLE I
THE EXPERIMENTAL RESULTS ON VAIHINGEN DATASETS.

Method	Backbone	Imp. surf.	Building	Low veg.	Tree	Car	Mean F1	OA (%)	mIoU (%)
U-Net [1]	-	84.331	86.479	73.132	83.886	40.825	73.731	82.023	61.362
ResUNet-a [2]	-	86.708	88.319	76.791	85.429	57.094	78.868	84.350	66.995
PSPNet [3]	ResNet34	90.273	94.218	82.757	88.606	51.100	81.391	88.820	71.591
DANet [5]	ResNet34	91.135	94.818	83.467	88.923	62.979	84.264	89.524	74.728
EaNet [7, 9]	ResNet34	92.172	95.197	82.811	89.254	80.563	87.999	89.995	80.223
CE-Net [11]	ResNet34	92.681	**95.529**	83.359	89.492	81.243	88.461	90.402	81.492
MAResU-Net	ResNet18	91.971	95.044	83.735	89.349	78.283	87.676	90.047	80.749
MAResU-Net	ResNet34	**92.912**	95.256	**84.947**	**89.939**	**88.330**	**90.277**	**90.860**	**83.301**

TABLE II
KAPPA Z-TEST COMPARING THE PERFORMANCE OF DIFFERENT METHODS.

Method	Kappa	KV (10^{-9})	ResUNet-a	PSPNet	DANet	EANet	CE-Net	MLAU-Net
U-Net	0.7682	3.1443	12.7608	39.5863	43.8255	47.5193	50.3952	52.8544
ResUNet-a	0.7993	2.7954	-	26.8824	31.1415	34.8537	37.7492	40.2256
PSPNet	0.8586	2.0706	-	-	4.2844	8.0201	10.9479	13.4527
DANet	0.8672	1.9586	-	-	-	3.7358	6.6662	9.1734
EaNet	0.8745	1.8598	-	-	-	-	2.9328	5.4420
CE-Net	0.8801	1.7861	-	-	-	-	-	2.5092
MAResU-Net	0.8848	1.7224	-	-	-	-	-	-

The computational demand for attention in memory and computation cost has significantly reduced thanks to LAM. Therefore, it is possible to directly model the global contextual dependencies of each pair of positions regardless of the size of the input, thereby enhancing the performance of the network in multiple stages. The superiority of the proposed MAResU-Net demonstrates that our method can capture refined and fine-grained features. The visual comparison is shown in Fig. 2 with the clear advantages in our method compared with other benchmarks.

2) Statistical Significance: To evaluate the statistical significance, we report Kappa z-test for pairwise methods based on Kappa coefficients of agreement and their variances using the following equation:

$$z = (k_1 - k_2)/\sqrt{v_1 + v_2}. \quad (13)$$

where k indicates the Kappa coefficient and v represents the Kappa variance. Specifically, if the value of z surpasses a threshold of 1.96, the two methods are regarded signally different at the 95 % confidence level. As can be seen from Table II, the classification accuracy of the proposed MAResU-Net is statistically higher than other comparative methods.

3) Ablation Study: As multi-stage attention blocks are utilized to exploit global contextual in the proposed MAResU-Net, it is valuable to conduct the ablation study and measure the impact of each block. As shown in TABLE III, the utilization of attention blocks boosts the classification performance dramatically compared with the baseline methods. Meanwhile, attention blocks at low levels contribute more than those at high levels.

TABLE III
THE ABLATION STUDY ABOUT THE ATTENTION BLOCK.

Method	Mean F1	OA (%)	mIoU
ResNet34	85.897	89.495	78.520
MAResU-Net 1	86.159	89.543	79.420
MAResU-Net 2	87.397	89.794	80.009
MAResU-Net 3	88.952	90.025	81.184
MAResU-Net 4	89.492	90.468	82.101
MAResU-Net	90.277	90.860	83.301

TABLE IV
THE INFORMATION ABOUT MODEL COMPLEXITIES.

Method	Train Time (s) / epoch	Inference Time (s)	Complexity (G)	Parameters (M)
U-Net	251	18.04	61.921	43.420
ResUNet-a	511	26.75	26.991	39.946
PSPNet	101	3.73	5.563	34.138
DANet	85	3.29	4.890	22.782
EaNet	108	7.19	7.107	44.341
CE-Net	124	6.51	8.988	29.005
MAResU-Net	135	7.10	8.772	26.277

4) Model Complexity: Considering the complexity of the model is significant to assess the merit of a framework, we report the training time for each epoch, inference time,

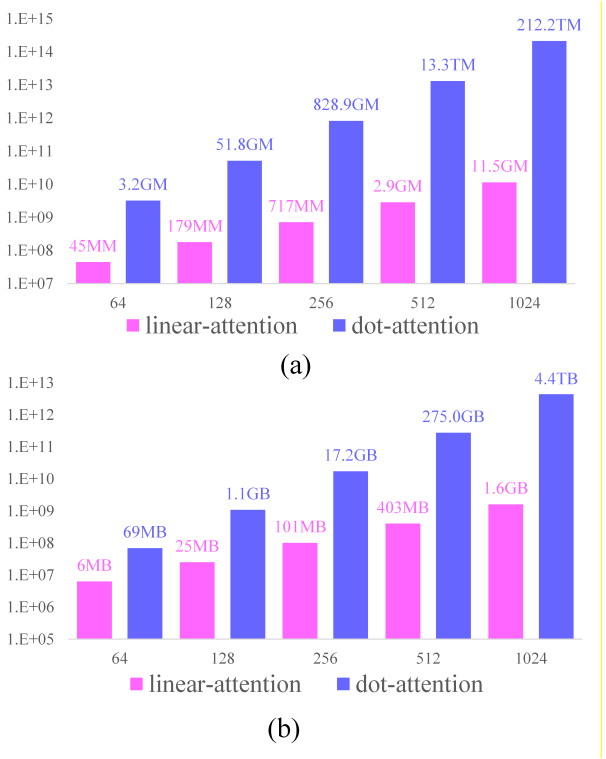

Fig. 3. The (a) computation requirement and (b) memory requirement under different input sizes. The calculation assumes $D = D_v = 2D_k = 64$. Please notice that the figure is in log scale.

complexity, and parameters in Table IV, which demonstrates that the design of MAResU-Net is computationally efficient.

The detailed comparison in terms of resource consumption between the linear attention and dot-attention is shown in Fig. 3. For a 64 × 64 × 64 input, the linear attention yields a 72-fold saving of computation (3 GMMACC to 45 MMACC) and 11-fold saving of memory (69MB to 6MB). With increased input size, the gap widens. For a 64 × 256 × 256 input, the dot-attention requires significant demand for computation (829 GMACC) and memory (17 GB), whereas the kernel attention only utilizes 1/1155 computation (717 MMACC) and 1/171 memory (101MB).

V. Conclusion

In this Letter, we propose a linear attention mechanism that reduces the complexity of the dot-product attention mechanism from $O(N^2)$ to $O(N)$. Based on the proposed LAM and the ResNet, we reconstruct the skip connections in the raw U-Net and proposed the MAResU-Net for semantic segmentation using fine-resolution remote sensing images. Experiments conducted on the Vaihingen dataset manifest the effectiveness of our MAResU-Net in both classification accuracy and computational efficiency.

Acknowledgments

The design of the method was inspired by Jianlin Su's blog in https://spaces.ac.cn/archives/7546 (04 Jul 2020).

Reference

[1] O. Ronneberger, P. Fischer, and T. Brox, "U-net: Convolutional networks for biomedical image segmentation," in *International Conference on Medical image computing and computer-assisted intervention*, 2015: Springer, pp. 234-241.

[2] F. I. Diakogiannis, F. Waldner, P. Caccetta, and C. Wu, "Resunet-a: a deep learning framework for semantic segmentation of remotely sensed data," *ISPRS Journal of Photogrammetry and Remote Sensing,* vol. 162, pp. 94-114, 2020.

[3] H. Zhao, J. Shi, X. Qi, X. Wang, and J. Jia, "Pyramid scene parsing network," in *Proceedings of the IEEE conference on computer vision and pattern recognition*, 2017, pp. 2881-2890.

[4] A. Vaswani *et al.*, "Attention is all you need," in *Advances in neural information processing systems*, 2017, pp. 5998-6008.

[5] J. Fu *et al.*, "Dual attention network for scene segmentation," in *Proceedings of the IEEE Conference on Computer Vision and Pattern Recognition*, 2019, pp. 3146-3154.

[6] X. Wang, R. Girshick, A. Gupta, and K. He, "Non-local neural networks," in *Proceedings of the IEEE conference on computer vision and pattern recognition*, 2018, pp. 7794-7803.

[7] R. Li, S. Zheng, C. Duan, Y. Yang, and X. Wang, "Classification of Hyperspectral Image Based on Double-Branch Dual-Attention Mechanism Network," *Remote Sensing,* vol. 12, no. 3, p. 582, 2020.

[8] R. Li and C. Duan, "ABCNet: Attentive Bilateral Contextual Network for Efficient Semantic Segmentation of Fine-Resolution Remote Sensing Images," *arXiv preprint arXiv:2102.02531,* 2021.

[9] X. Zheng, L. Huan, G.-S. Xia, and J. Gong, "Parsing very high resolution urban scene images by learning deep ConvNets with edge-aware loss," *ISPRS Journal of Photogrammetry and Remote Sensing,* vol. 170, pp. 15-28, 2020.

[10] R. Child, S. Gray, A. Radford, and I. Sutskever, "Generating long sequences with sparse transformers," *arXiv preprint arXiv:1904.10509,* 2019.

[11] Z. Gu *et al.*, "Ce-net: Context encoder network for 2d medical image segmentation," *IEEE transactions on medical imaging,* vol. 38, no. 10, pp. 2281-2292, 2019.

[12] N. Kitaev, L. Kaiser, and A. Levskaya, "Reformer: The Efficient Transformer," in *International Conference on Learning Representations*, 2019.

[13] A. Katharopoulos, A. Vyas, N. Pappas, and F. Fleuret, "Transformers are RNNs: Fast Autoregressive Transformers with Linear Attention," *arXiv preprint arXiv:2006.16236,* 2020.

[14] R. Li, S. Zheng, C. Duan, and J. Su, "Multi-Attention-Network for Semantic Segmentation of High-Resolution Remote Sensing Images," *arXiv preprint arXiv:2009.02130,* 2020.

[15] Z. Shen, M. Zhang, H. Zhao, S. Yi, and H. Li, "Efficient attention: Attention with linear complexities," in *Proceedings of the IEEE/CVF Winter Conference on Applications of Computer Vision*, 2021, pp. 3531-3539.

[16] C. Zhang, P. M. Atkinson, C. George, Z. Wen, M. Diazgranados, and F. Gerard, "Identifying and mapping individual plants in a highly diverse high-elevation ecosystem using UAV imagery and deep learning," *ISPRS J. Photogramm. Remote Sens.,* vol. 169, pp. 280-291, 2020.

[17] R. Li, C. Duan, S. Zheng, C. Zhang, and P. M. Atkinson, "MACU-Net for Semantic Segmentation of Fine-Resolution Remotely Sensed Images," *IEEE Geoscience and Remote Sensing Letters,* 2021.

[18] D. Bahdanau, K. Cho, and Y. Bengio, "Neural machine translation by jointly learning to align and translate," *arXiv preprint arXiv:1409.0473,* 2014.

[19] F. Yu and V. Koltun, "Multi-scale context aggregation by dilated convolutions," *arXiv preprint arXiv:1511.07122,* 2015.

[20] L.-C. Chen, G. Papandreou, I. Kokkinos, K. Murphy, and A. L. Yuille, "Semantic image segmentation with deep convolutional nets and fully connected crfs," *arXiv preprint arXiv:1412.7062,* 2014.

[21] H. Zhao *et al.*, "Psanet: Point-wise spatial attention network for scene parsing," in *Proceedings of the European Conference on Computer Vision (ECCV)*, 2018, pp. 267-283.

[22] Y. Yuan and J. Wang, "Ocnet: Object context network for scene parsing," *arXiv preprint arXiv:1809.00916,* 2018.

[23] H. Zhang, H. Zhang, C. Wang, and J. Xie, "Co-occurrent features in semantic segmentation," in *Proceedings of the IEEE Conference on Computer Vision and Pattern Recognition*, 2019, pp. 548-557.

[24] "ISPRS 2D semantic labeling contest." [Online]. Available: http://www2.isprs.org/commissions/comm3/wg4/semantic-labeling.html.